Chemical Engineering Journal 242 (2014) 19–26

Contents lists available at ScienceDirect

Chemical Engineering Journal

journal homepage: www.elsevier.com/locate/cej

An ethylenediamine-modified hypercrosslinked polystyrene resin: Synthesis, adsorption and separation properties

Xiaomei Wang [a,b], Kailiang Dai [b], Limiao Chen [a,c], Jianhan Huang [a,c,*], You-Nian Liu [a,c,*]

[a] College of Chemistry and Chemical Engineering, Central South University, Changsha, Hunan 410083, PR China
[b] Department of Bioengineering and Environmental Science, Changsha University, Changsha, Hunan 410003, PR China
[c] Key Laboratory of Resources Chemistry of Nonferrous Metals (Ministry of Education), Changsha, Hunan 410083, PR China

HIGHLIGHTS

- The ethylenediamine-modified hypercrosslinked resin was synthesized.
- The ethylenediamine-modified hypercrosslinked resins had different pore structure.
- The ethylenediamine-modified hypercrosslinked resins owned different polarity.
- The equilibrium and column breakthrough performance of the resin were determined.
- The separation performance of the resin from the mixed solution was measured.

ARTICLE INFO

Article history:
Received 21 October 2013
Received in revised form 10 December 2013
Accepted 14 December 2013
Available online 21 December 2013

Keywords:
Hypercrosslinked polystyrene resins
Adsorption
Equilibrium
Breakthrough
Phenol

ABSTRACT

We developed an effective approach for increasing phenol uptakes on a hypercrosslinked polystyrene resin and separating phenol from methyl orange or Congo red from the mixed solution. The ethylenediamine-modified hypercrosslinked polystyrene resins were synthesized, the equilibrium and breakthrough performance of the resins were determined on a selected resin named HJ-D33. The phenol uptakes on HJ-D33 were remarkably larger than that on its precursor and the commercial adsorbents like XAD-4, D301. The breakthrough capacity of phenol on HJ-D33 was 50.37 mg/ml wet resin at an initial concentration of 800.8 mg/L and a flow rate of 8.0 BV/h and the used HJ-D33 could be completely regenerated by a mixed solvent containing 0.01 mol/L of sodium hydroxide and 50% of ethanol. Methyl orange (or Congo red) and phenol could be dynamically separated by HJ-D33 resin column as the effluent was in the range of 0–60 BV.

1. Introduction

In 1969, Davankov and Tsyurupa proposed a fundamentally novel approach to obtain a kind of uniformly crosslinked polystyrene [1], and which leads to a creation of a so called "hypercrosslinked polystyrene" resin which had unique structure and extraordinary properties [2,3]. The hypercrosslinked polystyrene was proven an efficient polymeric adsorbent for adsorptive removal of aromatic compounds such as benzene, toluene and phenol from aqueous solutions. It was also widely applied as column packing materials in high-performance liquid chromatography (HPLC), ion size-exclusion chromatography materials and solid-phase extraction materials for gases, organic contaminants and organic vapors [4–6].

Hypercrosslinked polystyrene was generally prepared from a linear polystyrene or a low crosslinked polystyrene by adding typical bis-chloromethyl derivatives of aromatic hydrocarbons such as 1, 4-bis-(chloromethyl)-diphenyl, *p*-xylylenedichloride, 1, 4-bis-(*p*-chloromethylphenyl)-butane or 1, 3, 5-tris-(chloromethyl) mesitylene by a Friedel–Crafts reaction under the help of catalysts including anhydrous zinc chloride, iron (III) chloride or stannic (IV) chloride [7,8]. After the corresponding reaction, intensive networks with long-chain bridges between the initial polystyrene chains and the conformationally rigid links were formed accordingly, and which results in a major shift of the pore width distribution from predominately mesomacropores to meso/micropores distribution as well as a sharp increase of the Brunauer–Emmet–Teller (BET) surface area and pore volume [9,10].

Hypercrosslinked polystyrene can also be prepared from low crosslinked polystyrene using monochlorodimethyl ether as the crosslinking reagent according to two continuous steps. The first

* Corresponding authors at: College of Chemistry and Chemical Engineering, Central South University, Changsha, Hunan 410083, PR China.
E-mail addresses: jianhanhuang@csu.edu.cn (J. Huang), liuyounian@csu.edu.cn (Y.-N. Liu).

1385-8947/$ - see front matter © 2013 Elsevier B.V. All rights reserved.
http://dx.doi.org/10.1016/j.cej.2013.12.037

step contains a chloromethylation of the polystyrene under mild conditions and hence the chloromethylated polystyrene with quantitative chloromethyl groups will be achieved, the introduced chloromethyl groups can further react with another phenyl ring of the polystyrene by formation of an equivalent number of diphenylmethane-type rigid bridges through a typical Friedel–Crafts reaction, resulting in the post-crosslinking of the polystyrene and formation of hypercrosslinked polystyrene [11,12]. It was deemed that the residual chlorine content of the chloromethylated polystyrene reduced sharply after the Friedel–Crafts reaction [13]. In particular, it declined rapidly at the beginning and subsequently decreased slowly as the reaction proceeded, and hence the hypercrosslinked polystyrene with different residual chlorine content can be synthesized by regulating the Friedel–Crafts reaction time [13,14]. The residual chlorine content of the obtained hypercrosslinked polystyrene determines the pore structure and polarity of the products, and it is feasible to adjust the pore structure and polarity of the hypercrosslinked polystyrene by simply controlling the Friedel–Crafts reaction time. To the best of our knowledge, this approach for optimizing the hypercrosslinked polystyrene is little reported in the literature yet.

In this study, four hypercrosslinked polystyrene resins were synthesized from macroporous crosslinked chloromethylated polystyrene through the Friedel–Crafts reaction by regulating the Friedel–Crafts reaction time (0.5, 1.0, 3.0 and 5.0 h, respectively). These hypercrosslinked polystyrene resin were then chemically modified by an amination reaction with ethylenediamine to produce the ethylenediamine-modified hypercrossliked polystyrene. Thereafter, the adsorption selectivity of the resins towards phenol was confirmed by the batch adsorption, and the most promising resin HJ-D33 was selected for detailed experimental studies for adsorptive removal of phenol from aqueous solutions and separation of phenol from other molecules with larger molecular size such as methyl orange and Congo red.

2. Experimental

2.1. Materials

Macroporous crosslinked chloromethylated polystyrene was purchased from Langfang Chemical Co., Ltd., China, its crosslinking degree was 6%, chlorine content was measured to be 17.3%, its Brunauer–Emmett–Teller (BET) surface area was 28 m^2/g with an average pore width of 25.2 nm. Anhydrous iron (III) chloride, 1, 2-dichloroethane, ethylenediamine and ethanol was analytical reagents. Phenol (C_6H_5OH, Molecular weight (MW): 94.1), methyl orange ($C_{14}H_{14}N_3NaO_3S$, MW: 327.3) and Congo red ($C_{32}H_{22}N_6Na_2O_6S_2$, MW: 696.7) applied as the adsorbates were analytical reagents and used without further purification.

2.2. Synthesis of ethylenediamine-modified hypercrosslinked polystyrene resins

Ethylenediamine-modified hypercrosslinked polystyrene resin was synthesized by two continuous steps (Scheme S1). One is Friedel–Crafts reaction of macroporous crosslinked chloromethylated polystyrene, which performed by a similar procedure in Refs. [13,15], the hypercrosslinked polystyrene resin was obtained in this step, and the other is amination reaction of the hypercrosslinked polystyrene resin. Typically, 1, 2-dichloroethane was applied as the solvent to swell macroporous crosslinked chloromethylated polystyrene at room temperature for 24 h. Catalytic amounts of anhydrous iron (III) chloride was used as the catalysts. After refluxing reaction mixture for 0.5 h, 1 h, 3 h and 5 h, respectively, the hypercrosslinked polystyrene resins named HJ-05, HJ-11, HJ-33 and HJ-55 was obtained. After rinsing, the hypercrosslinked polystyrene resins were mixed with superfluous ethylenediamine and the reaction mixture was kept at 393 K for 20 h, and hence the ethylenediamine-modified hypercrosslinked polystyrene resins were prepared (labeled as HJ-D05, HJ-D11, HJ-D33 and HJ-D55).

2.3. Characterization of the resins and analysis of the adsorbates

The pore structure of the resins in the dry state such as the BET surface area, Langmuir surface area, t-plot micropore surface area, pore volume, t-plot micropore volume, average pore width and pore width distribution of the resins were determined by the N_2 adsorption and desorption isotherms at 77 K using a Micromeritics Tristar 3000 surface area and porosity analyzer. The total surface area and pore volume of the resins were calculated according to BET model while the t-plot micropore surface area and t-plot micropore volume were calculated by the Barrett, Joyner and Halenda (BJH) method, the pore width distribution of the meso/macroporus region of the resins was determined by applying BJH method to the N_2 desorption data, while the pore width distribution of the microporous region of the resin was determined by density functional theory (DFT) (Model: Carbon, Slit pores; Method: Non-negative regularization; No Smoothing, Standard deviation of fit: 3.308 cm^3/g) method using a Micromeritics ASAP 2020 Physisorption Analyzer. The Fourier transform infrared spectroscopy (FT-IR) of the resins was collected by KBr disks on a Nicolet 510P Fourier transformed infrared instrument. The chorine content of the resins was measured by the Volhard method [16] and the weak basic exchange capacity of the resin was determined by another established method [17]. The morphology of the resins was carried out by scanning electron microscopy (SEM) performed on a JSM-6360LV SEM tester. The concentration of phenol, methyl orange and Congo red in aqueous solution was analyzed by UV analysis at the wavelength of 269.5, 463.5 and 498.0 nm, respectively.

2.4. Equilibrium adsorption

About 0.1000 g of the resin was accurately weighed and mixed with 50 ml phenol aqueous solution at an initial concentration of about 100, 200, 300, 400 and 500 mg/L in a conical flask. 1.0 mol/L of hydrochloric acid or 1.0 mol/L of sodium hydroxide was employed to adjust the solution pH. Sodium chloride and cadmium nitrate were used to investigate the salinity and heavy metal ion effect on the adsorption. The flasks were then continuously shaken in a thermostatic oscillator at a desired temperature (300, 305 or 310 K) until the adsorption equilibrium was reached. The equilibrium concentration of phenol C_e (mg/L) was calculated and the equilibrium phenol uptakes on the resin q_e (mg/g) was determined as:

$$q_e = (C_0 - C_e)V/W \quad (1)$$

where C_0 is the initial concentration (mg/L), V is the volume of the phenol aqueous solution (L) and W the mass of the resin (g).

2.5. Dynamic adsorption, desorption and separation

The resins were immersed in de-ionized water at room temperature for 24 h and then packed in a glass column (inner diameter: 16 mm) densely to assemble a resin column. In the dynamic adsorption experiment, the phenol aqueous solution at an initial concentration of 800.8 mg/L was passed through the resin column at a flow rate of 8.0 BV/h (1BV = 10 ml). In the dynamic separation experiment, a synthetic mixed solution containing a prepared solution containing 500.5 mg/L of phenol and 498.6 mg/L of methyl orange or 504.8 mg/L of phenol and 502.3 mg/L of Congo red was

passed through the resin column at a flow rate of 8.5 BV/h. The effluents from the resin column were continuously collected and the concentration of phenol as well as methyl orange or Congo red was simultaneously monitored until it approached the initial one. After the dynamic adsorption experiment, the resin column was roughly rinsed by 10 ml of de-ionized water and then a desorption solvent containing 0.01 mol/L of sodium hydroxide and 50% of ethanol was applied for the desorption process. 100 ml of the desorption solvent was passed through the resin column at a flow rate of 4.0 BV/h and the concentration of phenol was determined until it was about zero.

3. Results and discussion

3.1. Characteristics of the resins

After the Friedel–Crafts reaction, the chlorine content of the hypercrosslinked polystyrene resins HJ-05, HJ-11, HJ-33 and HJ-55 sharply decreased from 17.3% to 6.02%, 3.99%, 3.21% and 3.02%, respectively (Table 1), implying that the chlorine of the macroporous crosslinked chloromethylated polystyrene was consumed in the first step and a longer reaction time lead to lower chlorine content. After the amination reaction, the chlorine contents of the ethylenediamine-modified hypercrosslinked polystyrene resins HJ-D05, HJ-D11, HJ-D33 and HJ-D55 were further decreased and the final chlorine content of the resins was about 1.0%, which suggested that uploading of amino groups on the resins was performed successfully and the uploading amounts were quite different, HJ-D05 should have the highest uploading amount while HJ-D55 might own the least. Meanwhile, the weak basic exchange capacity of HJ-D05, HJ-D11, HJ-D33 and HJ-D55 was determined to be 2.24, 1.42, 1.03 and 0.88 mmol/g, respectively, confirming that substitution of chlorine by amino groups was successful and the obtained ethylenediamine-modified hypercrosslinked polystyrene resins possessed different polarity, HJ-D05 was the most polar resin while HJ-D55 was the least polar resin.

The BET surface area of HJ-05, HJ-11, HJ-33 and HJ-55 rapidly increased from 28.0 m^2/g to 784.8, 895.8, 901.3 and 918.8 m^2/g, respectively, meaning that a large quantity of methylene crosslinking bridges with conformationally rigid links were formed between the polystyrene chains in the Friedel–Crafts reaction and a longer reaction time brought about more methylene crosslinking bridges. In particular, the t-plot surface area and the t-plot micropore volume of the hypercrosslinked polystyrene resins accounted for more than half of the BET surface area and pore volume, which demonstrated that a large number of micropores were produced in the first step. After the amination reaction, the BET surface area, t-plot surface area, pore volume and t-plot pore volume of HJ-D05, HJ-D11, HJ-D33 and HJ-D55 are relatively reduced, this may be attributed to the fact that uploading of amino groups on the resins has partially made the pores collapsed.

As shown in Fig. 1, the N_2 uptakes of the resins was much larger than that of the chloromethylated polystyrene at the same relative pressure and all of the adsorption isotherms seemed close to type-II. At a relative pressure below 0.05 and above 0.95, the N_2 uptakes increased sharply with increasing of the relative pressure, demonstrating that micropores are predominant and macopores are also existent for the resins. The visible hysteresis loops of the desorption isotherm indicates that mesopores also exist. These analyses agree with results of the pore width distribution of the resins in Fig. S1. The Friedel–Crafts reaction results in a great transfer for the pore width distribution of the resins, meso/macropores are the main pores for the chloromethylated polystyrene, while mesopores in the range of 2–5 nm play a dominant role for the hypercrosslinked polystyrene resins as well as the ethylenediamine-modified hypercrosslinked polystyrene resins and few changes occur after the amination reaction.

After the Friedel–Crafts reaction, all of the vibrations of the hypercrosslinked polystyrene resins remained while the representative strong vibration of CH_2Cl groups at 1265 cm^{-1} was significantly weakened [18] (Fig. 2), which was in accordant with the sharp decreasing of the chlorine content. Simultaneously, a new moderate vibration appeared at 1705 cm^{-1} and this vibration may be assigned to the carbonyl groups stretching resulted from oxidation of CH_2Cl groups [12,19]. After the amination reaction, a strong and wide vibrational band appeared at 3438 cm^{-1} and this vibration was concerned with the N–H stretching of –NH–/–NH_2 groups of ethylenediamine [18]. Meanwhile, a vibrational band related to the N–H deformation was observed at 1511 cm^{-1}, another vibration associated with the C–N stretching was also arisen at 1103 cm^{-1}, which confirmed the successful uploading of ethylenediamine on the resins. The SEM images of the chloromethylated polystyrene, HJ-33 and HJ-D33 are presented in Fig. 3. It is interesting to observe that the surface of HJ-33 is much smoother than that of the chloromethylated polystyrene while the surface of HJ-D33 is a little rougher than HJ-33 [13,15].

3.2. Adsorption selectivity

Section 3.1 indicated that the four ethylenediamine-modified hypercrosslinked polystyrene resins had the different pore structure and polarity, HJ-D05 possessed the lowest BET surface area while the highest uploading amount of the amino groups, whereas HJ-D55 held the highest BET surface area while the lowest uploading amount of amino groups, indicative of their different adsorption selectivity. Fig. 4(a) compares the phenol uptakes of HJ-D05, HJ-D11, HJ-D33 and HJ-D55 from aqueous solutions, and it is obvious that the phenol uptakes on the resins firstly increased and then decreased with increment of the Friedel–Crafts reaction time and HJ-D33 had the largest phenol uptakes among the four resins. The BET surface area of HJ-D33 is much higher than that of HJ-D05 (difference: 279.3 m^2/g), while the weak basic exchange capacity of HJ-D33 is higher than that of HJ-D55 (difference 0.17 mmol/g). The higher BET surface area of HJ-D33 may result in a higher physical adsorption of phenol on the resins by Van der Waals forces [20], while the uploaded amino groups may cause

Table 1
The structural parameters of the hypercrosslinked polystyrene HJ-05, HJ-11, HJ-33 and HJ-55 and the ethylenediamine-modified hypercrosslinked polystyrene resins HJ-D05, HJ-D11, HJ-D33 and HJ-D55.

	HJ-05	HJ-11	HJ-33	HJ-55	HJ-D05	HJ-D11	HJ-D33	HJ-D55
BET surface area (m^2/g)	784.8	895.8	901.3	918.8	527.9	692.1	807.2	895.1
Langmuir surface area (m^2/g)	1156	1320	1336	1362	779.3	1027	1194	1323
t-Plot micropore surface area (m^2/g)	426.5	484.3	493.8	495.3	279.7	384.6	445.0	517.2
Pore volume (cm^3/g)	0.5033	0.5820	0.5751	0.6059	0.3627	0.4591	0.5242	0.5620
t-Plot micropore volume (cm^3/g)	0.2319	0.2636	0.2701	0.2712	0.1513	0.2103	0.2429	0.2811
Average pore width (nm)	2.56	2.59	2.55	2.63	2.74	2.65	2.59	2.51
Chlorine content (%)	6.02	3.99	3.21	3.02	1.05	0.98	1.01	0.84
Weak basic exchange capacity (mmol/g)	/	/	/	/	2.24	1.42	1.03	0.88

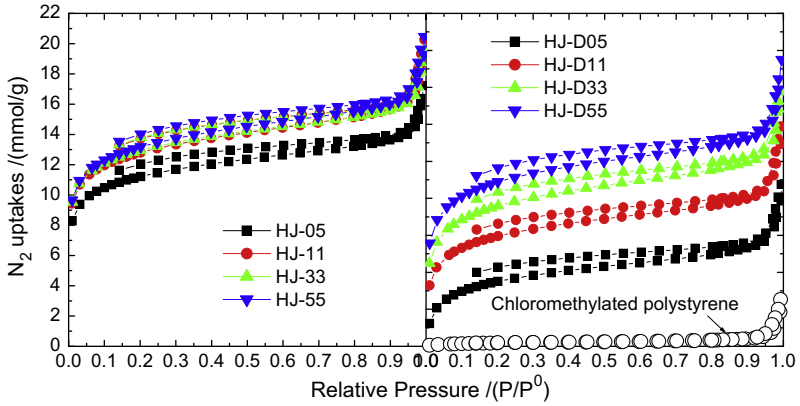

Fig. 1. N_2 adsorption and desorption isotherms of the hypercrosslinked polystyrene HJ-05, HJ-11, HJ-33 and HJ-55 (a) and ethylenediamine-modified hypercrosslinked polystyrene resins HJ-D05, HJ-D11, HJ-D33 and HJ-D55 (b).

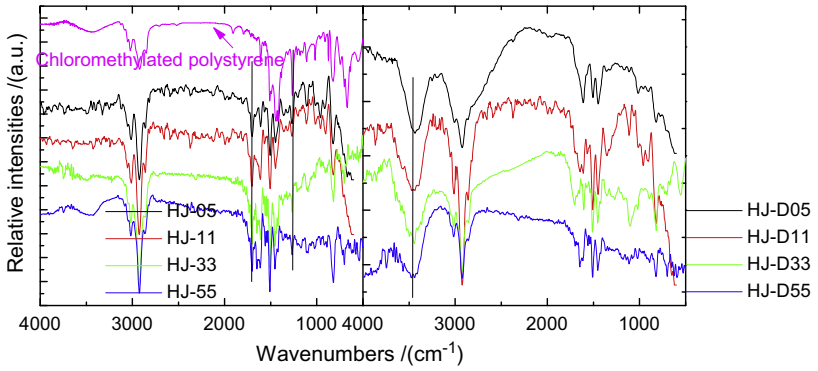

Fig. 2. FT-IR spectra of the hypercrosslinked polystyrene HJ-05, HJ-11, HJ-33 and HJ-55 as well as those of ethylenediamine-modified hypercrosslinked polystyrene resins HJ-D05, HJ-D11, HJ-D33 and HJ-D55.

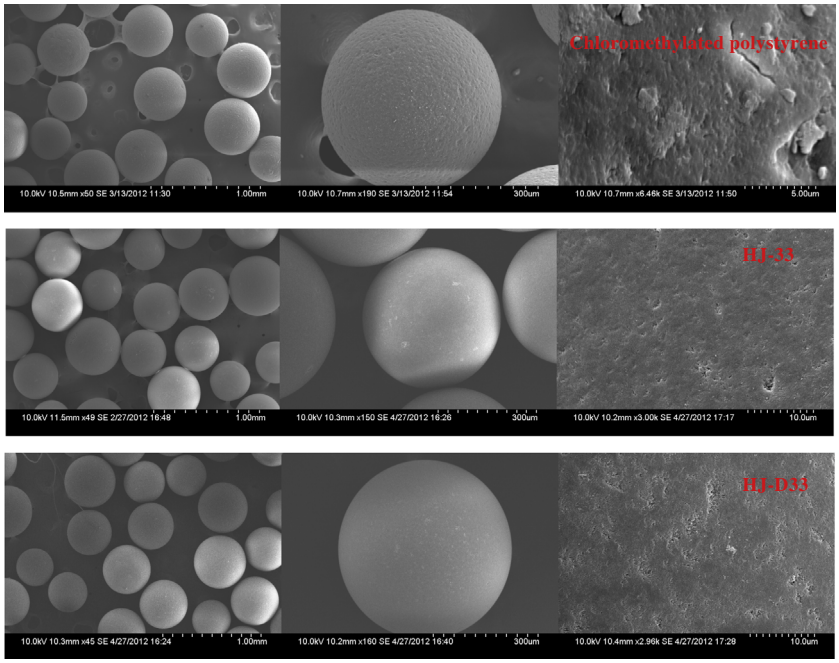

Fig. 3. Scanning electron microscopy (SEM) images of HJ-D33.

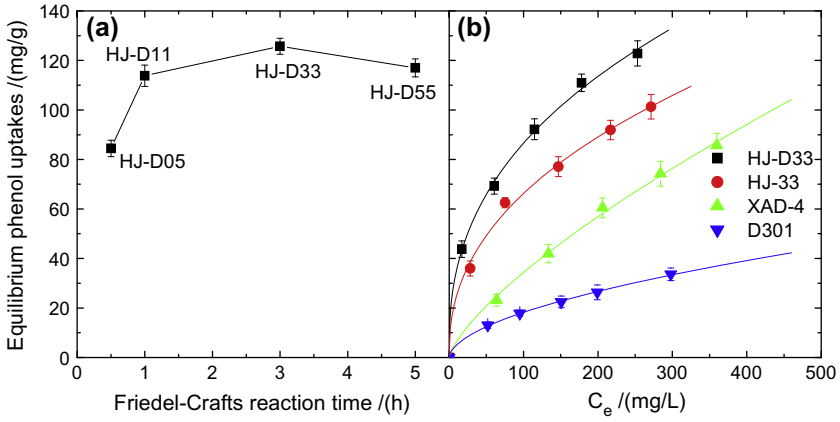

Fig. 4. (a) Comparison of equilibrium phenol uptakes on HJ-D05, HJ-D11, HJ-D33 and HJ-D55 from aqueous solutions; and (b) adsorption isotherms of phenol on HJ-33, HJ-D33, XAD-4 and D301 resin from aqueous solutions.

a chemical adsorption by acid–base interaction, hydrogen bonding, etc. [13,15,21]. As a result, combinations of the appropriate pore structure and the appropriate uploading amount of the amino groups make HJ-D33 a better resin for phenol adsorption.

Fig. 4(b) compares the phenol adsorption isotherms on HJ-33, HJ-D33, a commercial polystyrene resin XAD-4 and a commercial dimethylamine modified macroporous polystyrene resin D301 from aqueous solutions. At an equilibrium concentration of 100 mg/L, the phenol uptakes on HJ-33, HJ-D33, XAD-4 and D301 are measured to be 66.28, 86.59, 34.37 and 18.24 mg/g, respectively. Although the BET surface area of HJ-33 is relatively higher than that of HJ-D33 (difference: 94.1 m^2/g), the uploaded amino groups on HJ-D33 enhances the phenol adsorption due to the polarity matching [22,23]. This result demonstrates that chemical modification of hypercrosslinked polystyrene resin by introducing the amino groups on the resin is necessary and similar results are reported in some other papers [13,15]. In addition, as compared the phenol adsorption on HJ-D33 with some other adsorbents such as XAD-4-I (ketone carbonyl groups modified XAD-4 resin) [24], XAD-4-II (benzoyl groups modified XAD-4 resin) [24], DCX modified XAD-4 resin [25], BCMBP modified XAD-4 resin [25], HJ-M05 (a diethylenetriamine-modified hypercrosslinked resin) [26], HJ-L15 (a toluene-modified hypercrosslinked resin) [27], HJ-K01 (a methylamine modified hypercrosslinked resin) [28] and HJ-Z01 (a N-methylacetamide-modified hypercrosslinked resin) [29], it can be concluded that the XAD-4-series resins are inferior to HJ-D33 for the phenol adsorption and the modified hypercrosslinked polystyrene-type resins are comparable with HJ-D33.

3.3. Equilibrium adsorption

Fig. 5 displays the phenol adsorption isotherms on HJ-D33 with the temperature at 300, 305 and 310 K, respectively. The phenol uptakes increase with increasing of the equilibrium concentration and decrease with increment of the temperature, implying that the adsorption is an exothermic process [17,30].

Langmuir and Freundlich isotherms are two typical isotherms for describing the adsorption on adsorbents from aqueous solutions [31,32]. Langmuir was the first one proposing a coherent theory of adsorption on a flat surface based on a kinetic viewpoint, and the Langmuir isotherm assumes that the adsorption energy is constant over all adsorption sites, the adsorption on the surface is localized and each site can accommodate only one molecule [31]. Its linear equation can be given as:

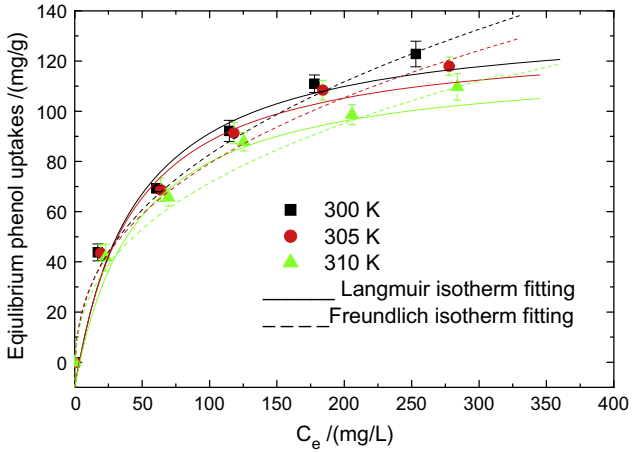

Fig. 5. Adsorption isotherms of phenol on HJ-D33 from aqueous solution at the temperature of 300, 305, 310 K, respectively.

$$C_e/q_e = C_e/q_m + 1/(q_m K_L) \quad (2)$$

where q_m is the monolayer uptakes (mg/g) and K_L is a constant related to adsorption energy (L/mg).

The Freundlich equation is one of the earliest empirical equations used to describe the equilibrium adsorption data, and it describes the adsorption on a heterogeneous surface and its linear form can be expressed as [32]:

$$\ln(q_e) = \ln K_f + (1/n)\ln C_e \quad (3)$$

where K_F [(mg/g)(L/mg)$^{1/n}$] and n are the characteristic constants.

The Langmuir and Freundlich isotherms were used to characterize the equilibrium isotherms by a linear and non-linear fitting method, the corresponding fitted curves by the non-linear fitting method are shown in Fig. 5, and the corresponding parameters such as q_m, K_L, K_F and n as well as the correlation coefficients R^2 by the linear fitting method are summarized in Table S1. Both of the Langmuir and Freundlich isotherms are shown to be suitable for fitting the isotherm data since $R^2 > 0.98$ and the Freundlich isotherm appears to be more appropriate for the isotherm data than the Langmuir isotherm due to $R^2 > 0.99$.

3.4. Effect of the solution pH on the adsorption

The phenol uptakes on HJ-D33 as a function of the solution pH are displayed in Fig. S2. It is evident that the phenol uptakes on HJ-D33 are very sensitive to the solution pH and they reach the

largest as the solution pH is in the range of 7.30–8.05. The phenol uptakes decrease about 15% at the solution pH < 6.0, and it decrease higher than 80% at the solution pH > 12.0. According to the reported pK_a of phenol (pK_a = 9.89) and pK_b of ethylenediamine (pK_b = 7.15), the dissociation curves of phenol as well as ethylenediamine in aqueous solution are predicted on dependency of the solution pH and the results are exhibited in Fig. S2. It is clear that the phenol adsorption on HJ-D33 has the same trend as the dissociation curve of phenol as the solution pH is ranged in 8.05–13.01, which indicates that the molecular form of phenol is favorable for the adsorption. Additionally, the phenol adsorption on HJ-D33 has the same tendency as the dissociation curve of ethylenediamine as the solution pH is decreased from 8.05 to 1.11, which further confirmed that ethylenediamine was uploaded on the resin successfully.

3.5. Effect of sodium chloride on the adsorption

Inorganic salts such as sodium chloride, sodium sulfate and so on are coexistent in the industrial phenol wastewater, sometimes the concentration of the inorganic salts possesses a very high level, which may have a negative effect on the resin adsorption. Therefore, the effect of sodium chloride on the ability of HJ-D33 for phenol adsorption is determined from aqueous solutions and the results are depicted in Fig. S3. It is observed that sodium chloride exhibits the positive effect on the phenol adsorption on HJ-D33, which may be from the so called "salting-out" effect.

3.6. Effect of Cd^{2+} on the adsorption

Heavy metals such as Hg^{2+}, Pb^{2+} and Cd^{2+} may coexist with the phenolic compounds in the wastewater. Cd^{2+} was chosen as a model heavy metal in this study and its effect on the phenol adsorption on HJ-D33 is examined. As can be seen from Fig. S4, the phenol uptakes change slightly with increasing of the concentration of Cd^{2+} as the concentration of Cd^{2+} is in the range of 0–10 mg/L, demonstrating that Cd^{2+} poses a slight effect on the phenol adsorption.

3.7. Dynamic adsorption and desorption

In the above sections, the phenol uptakes on HJ-D33 is shown to be quite large, enhanced with increasing of the concentration of sodium chloride and slightly changed with the concentration of Cd^{2+}, and it is hopeful that this resin has great application prospects for adsorptive removal of phenol from aqueous solution. Dynamic adsorption is a direct evaluation of an adsorbent's efficacy during the continuous column operation, hence the breakthrough characteristics of HJ-D33 towards phenol was tested in a fixed-bed experiment. For the column operation, the processing amount at the breakthrough point (breakthrough capacity) is the most important for judging whether the adsorbents can be applied in real field application or not. In this study, the breakthrough point was set to be C_v/C_0 = 0.05 and Fig. 6(a) indicated that the breakthrough point of phenol adsorption on HJ-D33 is 62.9 BV at an initial concentration of 800.8 mg/L and a flow rate of 8.0 BV/h, which is much higher than that of XAD-4 (28.2 BV) and HJ-33 (52.9 BV), respectively. The breakthrough capacity of phenol by XAD-4, HJ-33 and HJ-D33 can be calculated to be 22.58, 42.36 and 50.37 mg/ml wet resin, respectively, which confirms that HJ-D33 is an efficient polymeric adsorbent for adsorptive removal of phenol from aqueous solutions.

After the dynamic adsorption, the HJ-D33 resin column was roughly rinsed by 10 ml of de-ionized water and different desorption solvents were then employed for the desorption process, and the recovery ratio of the resin was depicted in Fig. 7(a). It is found that water can hardly purge the resin column and only 6.25% of phenol is desorbed from the resin column as water is utilized as the desorption solvent. 0.01 mol/L of sodium hydroxide aqueous solution can partly desorb phenol from the resin column and 75.6% of phenol is desorbed from the resin column, which in turn confirms the correctness of the results of solution pH on the adsorption. Ethanol aqueous solution can practically cleanse the resin column and 50.3% of the recovery ratio is achieved as 50% of ethanol aqueous solution is used. In particular, a mixed solution between sodium hydroxide and ethanol can greatly improve the recovery ratio of the resin and 99.6% of the recovery ratio is achieved as a mixed solution of 0.01 mol/L of sodium hydroxide and 50% of ethanol is employed hence it was applied for the desorption process in the current study. At a flow rate of 4.0 BV/h, 100 ml of the desorption solvent was passed through the resin column, only 6.0 bed volumes of the desorption solvent was needed to completely regenerate the resin column and the dynamic desorption uptakes were determined to be 624.3 mg (Fig. 6(b)), which was very close the saturated dynamic uptakes (630.9). The HJ-D33 resin was used repeatedly (Fig. 7(b)) and the phenol uptakes decreased to approximately 97.2% after five cycles of adsorption–desorption process, exhibiting an excellent reusability and remarkable regeneration.

3.8. Dynamic separation of phenol from the mixed solution

Micropores were predominant for HJ-D33, which gives a promise of separation of the organic compounds with different molecular size by molecular sieving effect. However, the pore width distribution of HJ-D33 in the microporous region is missing, and hence the pore width distribution of HJ-D33 was further determined by DFT method using a Micromeritics ASAP 2020 Physisorption Analyzer and the results are shown in Fig. S5. Fig. S5 agrees with Fig. S1 in the meso/macroporous region while it possesses a more explicit pore width distribution in the microporous region. It seems that the pores below 2 nm are the most predominant pores for HJ-D33, which confirm its possibility for separation of organic compounds with different molecular size [33]. The molecules with small molecular size can diffuse into the pores of the resin and the adsorption occurs normally, while the molecules with large molecular size cannot pass through the pores of the resin favorably, resulting in a smaller uptakes and even no adsorption.

In this study, three model molecules with different molecular size such as phenol, methyl orange and Congo red were selected and firstly the isotherms of the three adsorbates were respectively measured and the results are shown in Fig. 8(a). The phenol uptakes on HJ-D33 are the largest while the Congo red uptakes are the smallest, which follows an order as: $q_{e\,(\text{phenol})} > q_{e\,(\text{methyl orange})} > q_{e\,(\text{Congo red})}$. The molecular sizes of phenol, methyl orange and Congo red are predicted to be 0.58 nm, 1.19 nm and 2.29 nm, respectively, which has an order as: phenol < methyl orange < Congo red, and the molecular size of Congo red is almost equal to the average pore diameter of HJ-D33. In conclusion, the adsorbate with the largest molecular size (Congo red) possesses the smallest uptakes on HJ-D33 while the adsorbate with the smallest molecular size (phenol) has the largest uptakes, suggesting a potential molecular sieving effect of HJ-D33 for the three adsorbates [15,33]. Some relatively large micropores (>1.2 nm), mesopores (2–50 nm) as well as macropores (>50 nm) were found for HJ-D33, which are responsible for the methyl orange adsorption. As for Congo red, only the macropores (>2.5 nm) are accessible and useful, so its uptakes are the smallest.

Furthermore, the dynamic adsorption of HJ-D33 from the mixed solution between phenol and methyl orange or phenol and Congo red were measured and the results are displayed in Fig. 8(b). Fig. 8(b) indicates that the breakthrough point phenol, methyl orange and Congo red on HJ-D33 are quite different from the

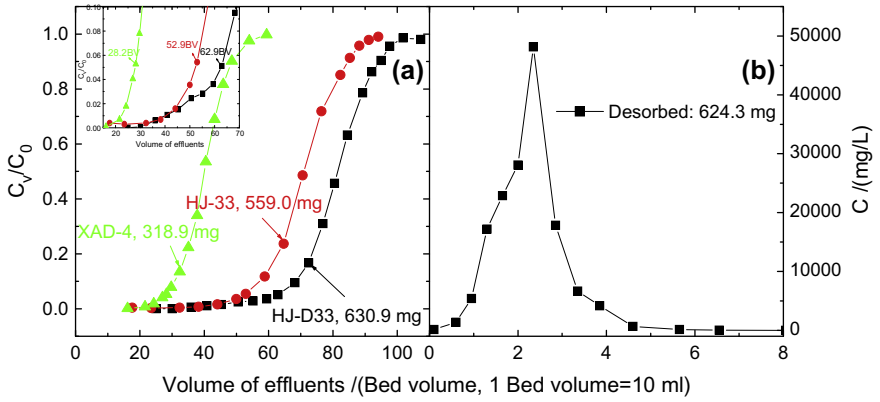

Fig. 6. (a) Dynamic adsorption curves of phenol adsorption on XAD-4, HJ-33 and HJ-D33 resin column with the initial concentration of 800.8 mg/L and a flow rate of 8.0 BV/h; and (b) dynamic desorption curves of phenol from HJ-D33 resin column as a mixed solution of 0.01 mol/L of sodium hydroxide and 50% of ethanol is employed as the desorption solvent.

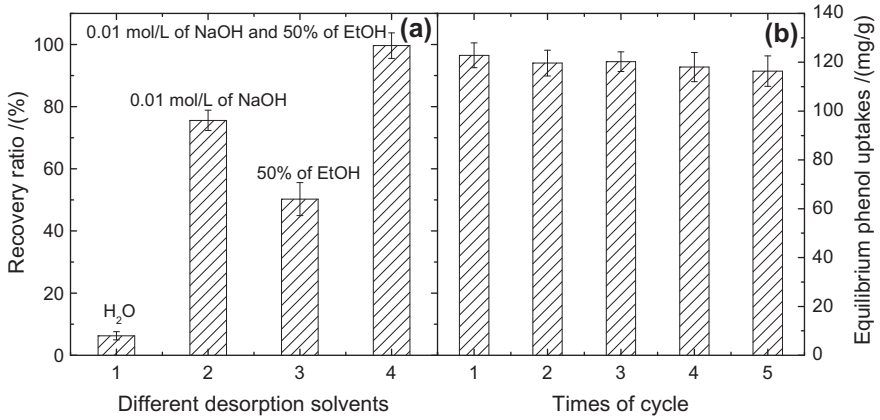

Fig. 7. (a) Recovery efficiency of different solvents for phenol desorption from HJ-D33 resin column; and (b) effect of the regeneration cycles on the phenol uptakes on HJ-D33.

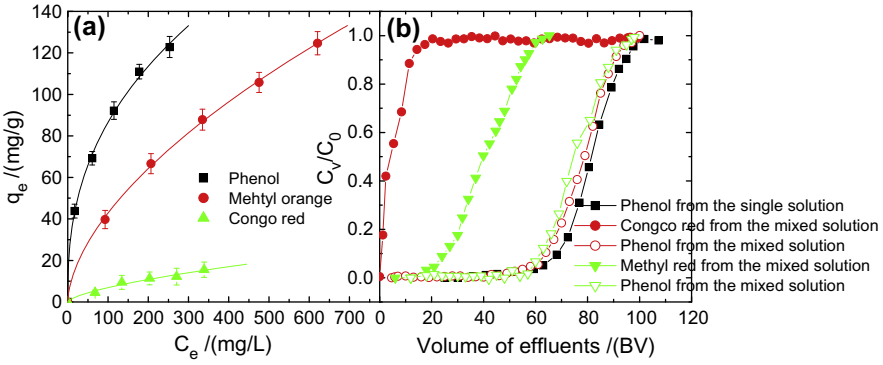

Fig. 8. (a) Adsorption isotherms of phenol, methyl orange and Congo red on HJ-D33 resin from aqueous solutions; and (b) dynamic adsorption and separation of phenol and methyl orange as well as phenol and Congo red. (For interpretation of the references to color in this figure legend, the reader is referred to the web version of this article.)

mixed solution. The breakthrough point of methyl orange was measured to be 21 BV, which was much lower than that of phenol (60 BV). That is HJ-D33 can separate methyl orange from phenol as the effluent is in the range of 21–60 BV. Congo red cannot be adsorbed on HJ-D33 and it is leaked out directly after starting the dynamic adsorption experiment while phenol does not leaked out until 60 BV, so HJ-D33 can separate Congo red from phenol as the effluent ranges from 0 to 60 BV.

4. Conclusion

Four ethylenediamine-modified hypercrosslinked polystyrene resins HJ-D05, HJ-D11, HJ-D33 and HJ-D55 were prepared by controlling the Friedel–Craft reaction time and they were shown to possess different pore textural property and surface functionality, indicative of their different adsorption selectivity towards phenol. HJ-D33 had the highest phenol uptakes among the four resins and

it was superior to its precursor HJ-33 and many other commercial resins. The Langmuir and Freundlich isotherms correlated well the phenol isotherms and Freundlich isotherm characterized better. At an initial concentration of 800.8 mg/L and a flow rate of 8.0 BV/h, the breakthrough capacity of phenol on HJ-D33 was 50.37 mg/ml wet resin, which were much higher than that of XAD-4 (22.58 mg/ml wet resin) and HJ-33 (42.36 mg/ml wet resin). The HJ-D33 resin column loaded by phenol could be regenerated by 60 ml of 0.01 mol/L of sodium hydroxide and 50% of ethanol aqueous solution completely and the phenol uptakes decreased to approximately 97.2% after five cycles of adsorption–desorption process. HJ-D33 could separate methyl orange from phenol as the effluent was in the range of 21–60 BV and it could separate Congo red from phenol as the effluent ranges from 0 to 60 BV.

Acknowledgments

The National Natural Science Foundation of China (Nos. 21174163, 21376275), the Shenghua Yuying Project of Central South University are gratefully acknowledged.

Appendix A. Supplementary material

Supplementary data associated with this article can be found, in the online version, at http://dx.doi.org/10.1016/j.cej.2013.12.037.

References

[1] S.V. Rogozhin, V.A. Davankov, M.P. Tsyurupa, Patent USSR 299165, 1969.
[2] A. Tadim, V.A. Davankov, M.P. Tsyurupa, Structure and properties of porous hypercrosslin ked polystyrene sorbents 'Styrosorb', Pure Appl. Chern. 61 (1989) 1881–1888.
[3] V.A. Davankov, M.P. Tsyurupa, Structure and properties of hypercrosslinked polystyrene polystyrene-the first representative of a new class of polymer networks, React. Polym. 13 (1990) 27–42.
[4] M.P. Tsyurupa, V.A. Davankov, Porous structure of hypercrosslinked polystyrene polystyrene: state-of-the-art mini-review, React. Funct. Polym. 66 (2006) 768–779.
[5] V. Davankov, M. Tsyurupa, Preparative frontal size-exclusion chromatography of mineral ions on neutral hypercrosslinked polystyrene, J. Chromatogr. A 1087 (2005) 3–12.
[6] V. Davankov, M. Tsyurupa, M. Ilyin, L. Pavlova, Hypercross-linked polystyrene and its potentials for liquid chromatography: a mini-review, J. Chromatogr. A 965 (2002) 65–73.
[7] V.A. Davankov, S.V. Rogozhin, M.P. Tsyurupa, Macronet isoporous gels through crosslinking of dissolved polystyrene, J. Polym. Sci. Symp. 47 (1974) 95–101.
[8] M.P. Tsyurupa, V.A. Davankov, Hypercrosslinked polystyrene polymers: basic principle of preparing the new class of polymeric materials, React. Funct. Polym. 53 (2002) 193–203.
[9] A.M. Li, Q.X. Zhang, G.C. Zhang, J.L. Chen, Z.H. Fei, F.Q. Liu, Adsorption of phenolic compounds from aqueous solutions by a water-compatible hypercrosslinked polystyrene polymeric adsorbent, Chemosphere 47 (2002) 981–989.
[10] X.H. Yuan, X.H. Li, E.B. Zhu, J. Hu, W.C. Sheng, S.S. Cao, A novel hypercrosslinked polystyrene polymeric adsorbent modified by phenolic hydroxyl group of 2-naphthol with bromoethane as crosslinking reagent, Carbohydr. Polym. 74 (2008) 468–473.
[11] J.H. Huang, K.L. Huang, S.Q. Liu, A.T. Wang, C. Yan, Adsorption of Rhodamine B and methyl orange on a hypercrosslinked polystyrene polymeric adsorbent in aqueous solutions, Colloids Surf. A 330 (2008) 55–61.
[12] M.C. Xu, Z.Q. Shi, B.L. He, Structure and adsorption properties of hypercrosslinked polystyrene adsorbents, Acta Polym. Sinica. 4 (1996) 446–449.
[13] J.H. Huang, X.Y. Jin, J.L. Mao, B. Yuan, R.J. Deng, S.G. Deng, Synthesis, characterization and adsorption properties of diethylenetriamine-modified hypercrosslinked resins for efficient removal of salicylic acid from aqueous solution, J. Hazard. Mater. 217–218 (2012) 406–415.
[14] J.H. Ahn, J.E. Jang, C.G. Oh, S.K. Ihm, J. Cortez, D.C. Sherrington, Rapid generation and control of microporosity, bimodal pore size distribution, and surface area in davankov-type hyper-cross-linked resins, Macromolecules 39 (2006) 627–632.
[15] Y. Li, R.F. Cao, X.F. Wu, J.H. Huang, S.G. Deng, X.Y. Lu, Hypercrosslinked poly(styrene-co-divinylbenzene) resin as a specific polymeric adsorbent for purification of berberine hydrochloride from aqueous solutions, J. Colloid Interface Sci. 400 (2013) 78–87.
[16] C.P. Wu, C.H. Zhou, F.X. Li, Experiments of Polymeric Chemistry, Anhui Science and Technology Press, Hefei, 1987.
[17] B.L. He, W.Q. Huang, Ion Exchange and Adsorption Resin, Shanghai Science and Technology Education Press, Shanghai, 1995.
[18] J.T. Wang, Q.M. Hu, B.S. Zhang, Y.M. Wang, Organic Chemistry, Nankai University Press, Tianjing, 1998.
[19] G.H. Meng, A.M. Li, W.B. Yang, F.Q. Liu, X. Yang, Q.X. Zhang, Mechanism of oxidative reaction in the postcrosslinking of hypercrosslinked polystyrene polymers, Eur. Polym. J. 43 (2007) 2732–2737.
[20] M.S. Bilgili, Adsorption of 4-chlorophenol from aqueous solutionss by xad-4 resin: Isotherm, kinetic, and thermodynamic analysis, J. Hazard. Mater. 137 (2006) 157–164.
[21] H.T. Li, M.C. Xu, Z.Q. Shi, B.L. He, Isotherm analysis of phenol adsorption on polymeric adsorbents from nonaqueous solutions, J. Colloid Interface Sci. 271 (2004) 47–54.
[22] C.G. Oh, J.H. Ahn, S.K. Ihm, Adsorptive removal of phenolic compounds by using hypercrosslinked polystyrene polystyrenic beads with bimodal pore size distribution, React. Funct. Polym. 57 (2003) 103–111.
[23] D.M. Ruthven, Principles and Adsorption Processes, Willey Inter-science, New York, 1984.
[24] C.Y. Li, M.W. Xu, X.C. Sun, S. Han, X.F. Wu, Y.N. Liu, J.H. Huang, S.G. Deng, Chemical modification of Amberlite XAD-4 by carbonyl groups forphenol adsorption from wastewater, Chem. Eng. J. 229 (2013) 20–26.
[25] J.H. Huang, L. Yang, X.F. Wu, M.W. Xu, Y.N. Liu, S.G. Deng, Phenol adsorption on α, α′-dichloro-p-xylene (DCX) and 4,4′-bis(chloromethyl)-1,10-biphenyl (BCMBP) modified XAD-4 resins from aqueous solutions, Chem. Eng. J. 222 (2013) 1–8.
[26] J.H. Huang, H.W. Zha, X.Y. Jin, S.G. Deng, Efficient adsorptive removal of phenol by a diethylenetriamine-modified hypercrosslinked styrene-divinylbenzene (PS) resin from aqueous solution, Chem. Eng. J. 195–196 (2012) 40–48.
[27] J.H. Huang, R.J. Deng, K.L. Huang, Equilibria and kinetics of phenol adsorption on a toluene-modified hyper-cross-linked poly(styrene-co-divinyl benzene) resin, Chem. Eng. J. 171 (2011) 951–957.
[28] C.L. He, J.H. Huang, J.B. Liu, L.B. Deng, K.L. Huang, Methylamino groups modified hyper-crosslinked polystyrene resin for removal of phenol from aqueous solution, J. Appl. Polym. Sci. 119 (2011) 1435–1442.
[29] J.H. Huang, X.Y. Jin, S.G. Deng, Phenol adsorption on an N-methylacet- amide-modified hypercrosslinked resin from aqueous solutions, Chem. Eng. J. 192 (2012) 192–200.
[30] D.D. Duong, Adsorption Analysis: Equilibria and Kinetics, World Scientific Publishing, Singapore, 1998.
[31] I. Langmuir, The constitution and fundamental properties of solids and liquids. Part I. Solids, J. Am. Chem. Soc. 38 (1916) 2221–2295.
[32] H.M.F. Freundlich, Über die adsorption in lösungen, Z. Phys. Chem. 57A (1906) 385–470.
[33] J.H. Huang, Molecular sieving effect of a novel hyper-cross-linked resin, Chem. Eng. J. 165 (2010) 265–272.